677

PROPOSAL

TO STUDY THE SPIN DEPENDENCE IN THE INCLUSIVE PRODUCTION OF LAMBDA PARTICLES WITH THE POLARIZED BEAM AT FERMILAB.

by

R. Ditzler, D. Hill, H. Spinka, K. Toshioka,
D. Underwood and A. Yokosawa

Argonne National Laboratory, Argonne, Illinois

Y. Hemmi, R. Kikuchi, K. Miyake, T. Nakamura, K. Nishimura and N. Tamura

Kyoto University, Kyoto, Japan

H. Azaïez, K. Kuroda, A. Michalowicz, D. Perret-Gallix

LAPP, Annecy, France

G. Shapiro

Lawrence Berkeley Laboratory
University of California, Berkeley, California

D. H. Miller and C. LeRoy

Northwestern University, Evanston, Illinois

M. Corcoran, H. E. Miettinen, T. A. Mulera, G. S. Mutchler,
G. C. Phillips and J. B. Roberts

Rice University, Houston, Texas

A. DeLesquen and L. Van Rossum

Saclay, France

V. Apokin, Y. Matulenko, A. Meschanin, S. Nurushev,
V. Solovyanov and A. Vasilyev

Serpukhov, USSR

R. Birsa, F. Bradamante, S. Dalla Torre-Colautti, M. Giorgi, L. Lanceri,
A. Martin, P. Moras, A. Penzo, P. Schiavon and A. Villari

INFN, Sezione di Trieste, Trieste, Italy

DIRECTOR'S OFFICE

FEB 2 1981

January 30, 1981

Scientific Spokesman:
Aldo Penzo
CERN, E.P. Division
Geneva, Switzerland

ABSTRACT

Lambda particles are produced at large p_t and high energy with an important polarization transverse to the production plane, thus suggesting relevant spin effects at the level of constituents.

We propose to use the Fermilab polarized beam for a detailed study of the spin dependence in the production of lambda and other neutral strange particles by measuring the analyzing power and spin correlation parameters.

TABLE OF CONTENTS

ABSTRACT ii

page

1. INTRODUCTION 1
2. PHYSICS MOTIVATIONS 2
3. PRINCIPLE OF MEASUREMENT 4
4. EXPERIMENTAL METHODS 5
5. APPARATUS AND EXPERIMENTAL RESOLUTION 7
6. TRIGGER CRITERIA AND ON-LINE SELECTION 9
7. ACCEPTANCE EVALUATION AND BACKGROUND ESTIMATES 10
8. ESTIMATES OF RATES AND ASYMMETRY PRECISION 12
9. PLAN OF THE EXPERIMENT 13

REFERENCES 15

Figure captions 17

TABLES 18

1. INTRODUCTION

Measurements at Fermilab (1) have shown that lambda particles produced at p_t close to 2 Gev/c at 300 and 400 Gev/c off nuclei and liquid hydrogen have an important polarization P_0.

It is now clear that this effect is present in a wide energy range (2) and the characteristic dependence on p_t and x, almost constant with energy, is somehow embarassing for perturbative QCD, which would involve vanishing polarization at high p_t.

Models recently proposed to explain such polarization are able for the moment to describe a few qualitative features. They however rely specifically on semi-classical arguments to justify the production of a polarized strange quark as a constituent of the final lambda particle and do not pretend to account for the underlying dynamical spin structure.

It is particularly important in this context to study the spin dependence of the production process also with polarized protons and antiprotons, by measuring the production asymmetry A_N and correlation parameters between the spin of the initial proton and the final lambda polarization, such as the depolarization tensor components D_{NN} and D_{LL} measured with respectively transversal and longitudinal initial and final spin orientations.

These measurements can be performed using the polarized proton (antiproton) beam planned in the M2 beam line for the fixed-target Tevatron program (3).

Lambda particles produced by polarized protons off a liquid hydrogen or nuclear target are identified by detecting the $\Lambda^0 \rightarrow p\pi^-$ decay products in a magnetic spectrometer. Their polarization is measured by studying the angular distribution of the decay protons and pions.

This investigation can be extended to triple-spin parameters by using a polarized target.

2. PHYSICS MOTIVATIONS

Measuring important spin effects at high energy implies a non trivial coincidence of specifically favourable experimental conditions and the presence of interaction mechanisms responsible for the spin dependence.

It is therefore particularly significant that the most remarkable spin effects at the highest energies have been discovered in hyperon production : the self-analyzing power of their parity-non-conserving decay gives a unique possibility of determining the high energy hyperon polarization. Although it is not yet clear what mechanisms are responsible for the large polarization observed, these reactions are obvious candidates for a deeper investigation of the spin dependence in the basic subprocesses involving hadron constituents. Each of these processes can give characteristic contributions and their relative importance might be deduced from the measurement of additional spin parameters in a wide kinematical range.

In terms of perturbative QCD, vanishing single-spin effects are predicted at large p_t in quark-quark scattering (4). However non-negligible contributions might come from processes with interacting gluons (5).

For strange particle production in proton-proton collisions, processes of gluon fusion are relatively more important at moderate $x_t = 2p_t/\sqrt{s}$, while quark-quark interactions dominate at larger x_t values ; gluon contributions might be enhanced in nuclear targets (6).

From measurements with a polarized beam new information would be obtained on gluon spin distributions which are not directly probed in polarized lepton deep-inelastic scattering.

Quark-antiquark annihilation terms (where polarization of the sea quarks is also involved (7)) might contribute appreciably to spin effects too.

For antiproton-proton collisions both gluon fusion and annihilation diagrams are important and their interest for lambda production has been

recently pointed out in theoretical papers (8), predicting important effects in helicity correlation parameters (Fig.1).

It might be premature to enforce a QCD interpretation on the existing polarization data, also in view of the p_t range, still modest for a genuinely perturbative regime; however the process $pp \to \Lambda^0(\uparrow)X$ naturally accomodates a quark-based interpretation, as the Λ^0 wave function has the non-strange quarks in a singlet state and therefore the spin of the hyperon is carried by the strange quark.

Non-perturbative models based on confinement effects (9) or soft processes (10) account for the qualitative aspects of the observed Λ^0 polarization and for the relative behaviour of the production of $\bar{\Lambda}^0$, p , Ξ^0 , Σ^0 and Σ^+ (according to their SU(6) wave functions).

However such models are rather speculative about the nature of the process :

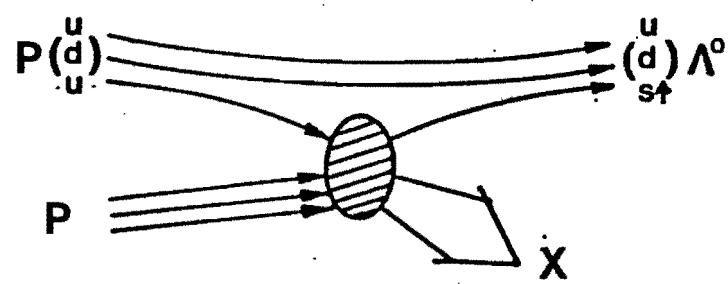

whereby a u-quark in the beam proton interacts with the target proton to produce a polarized s-quark in the final Λ^0. The large observed polarization implies that this interaction should generate a phase difference between spin-dependent elementary amplitudes, whose structure can be clarified by measurements with a polarized beam.

For example data on A_N , P_0 and D_{NN} at 6. Gev/c obtained at Argonne (11) for $pp \to \Lambda^0 X$ in the fragmentation region have been analyzed in terms of a Mueller-Regge model to individuate odd- and even-signature exchange contributions (12).

Similarly, combined measurements of this type at much higher energies and in a larger p_t interval would probe in detail the nature of the interaction between the constituents.

Further interesting results can be obtained using a polarized target in conjunction with the polarized beam, giving access to the determination of spin correlation parameters in the initial state and of higher rank tensors by triple-spin measurements.

3. PRINCIPLE OF MEASUREMENT

Experiments with a polarized beam and liquid hydrogen target have the advantage that spin parameters of inclusive reactions are directly reflected in the raw measured asymmetries, avoiding the large dilution factor introduced by the unpolarized material contained in standard polarized targets.

In this respect the process of Λ^0 production is particularly favourable, as both single- and double-spin measurements can be performed in clean experimental conditions.

With transversally polarized beam the differential cross-section depends also on the azimuthal angle ϕ and the spin dependent parameters are obtained from the study of the corresponding angular distributions :

$$\sigma(x,p_t^2,\phi) = \frac{1}{2\pi}\,\sigma_0(x,p_t^2)\,\left[\,1 + A_N(x,p_t^2)\,\vec{P}_B\cdot\hat{n}\,\right]$$

$$(\vec{P}_\Lambda\cdot\hat{n})\,\sigma(x,p_t^2,\phi) = \frac{1}{2\pi}\,\sigma_0(x,p_t^2)\,\left[P_0(x,p_t^2) + D_{NN}(x,p_t^2)\,\vec{P}_B\cdot\hat{n}\right]$$

where $\hat{n}$ is the normal to the production plane, $\vec{P}_B$ is the beam polarization, $\vec{P}_\Lambda$ is the final Λ^0 polarization and $\sigma_0(x,p_t^2)$ is the spin-averaged cross-section.

A_N is obtained by alternating the sign of the beam polarization and measuring the rate asymmetry at fixed production angle; additionally (also as a countercheck against systematic errors) the left-right asymmetry with respect to the beam direction can be measured.

P_0 is the part of the final Λ^0 polarization which is independent of the beam polarization and D_{NN} is the fraction of the initial beam polarization which is retained by the final particle.

In the case of longitudinally polarized beam the analogous component is given by D_{LL} .

The determination of these parameters requires the measurement of the components of the Λ^0 polarization as obtained by the decay proton angular distribution in the Λ^0 rest frame :

$$W\ (\theta^*, \phi^*) = (1/4\pi)\ [\ 1 + \alpha_\Lambda\ \hat{p}^* \cdot \vec{P}_\Lambda\ ]$$

In practice these spin-dependent parameters will be obtained via maximum likelihood fits to the same data.

Simultaneously with the $pp \to \Lambda^0 X$ measurements also data on K^0 production would be obtained as a by-product, providing a measurement of the analyzing power A_N for $pp \to K^0 X$.

Using a photon detector some interesting information might be gathered also for the production asymmetry in Σ^0 and Ξ^0 production.

4. EXPERIMENTAL METHODS

Measurements of high-energy Λ^0 particles rely on the determination of the decay pair $p\ \pi^-$, within a large background of associated particles.

The momentum distribution in the pair is very asymmetric as the proton takes on the average most of the Λ^0 momentum and is emitted in the laboratory within a narrow cone around the Λ^0 direction (Fig.2) .

The range of momenta and decay angles in the laboratory are :

for the p : $0.72\ p_\Lambda \leq p_p \leq 0.90\ p_\Lambda$; $0. \leq \theta_p \leq 124./p_\Lambda$ (mrad)

for the π^- : $0.23\ p_\Lambda \geq p_\pi \geq 0.06\ p_\Lambda$; $0. \leq \theta_\pi \leq 679./p_\Lambda$ (mrad)

Our detection criteria are based therefore on resolving preliminarly the p π^- pair in a large acceptance spectrometer and further determining the proton in a dedicated small-aperture high-resolution spectrometer, with a largely reduced background of associated particles [1].

Triggering schemes involve the definition of the accepted regions for protons and pions from Λ^0 decay by scintillation counter hodoscopes and their tagging by Cerenkov counters.

The requirement that the charged multiplicity is incremented by two between the target and the entrance of the first magnet is implemented by hit counting and dE/dx measurements.

The direction and the momenta of the produced particles are determined by proportional and drift chambers before and after the magnets.

Information from the chambers is fed to on-line processors, to calculate points in space and correlate tracks in the two spectrometers, thus greatly reducing the background from directly produced charged particles.

The off-line program will search for lambda particles following the most appropriate criteria in order to minimize the complexity of the track-finding and event reconstruction procedure. For example high-momentum positive trajectories measured in the second spectrometer are attributed to 'protons' and traced back into the decay region. Negative trajectories intersecting the 'proton' track within a cone compatible with the maximum opening angle from Λ^0 decay are then attributed to 'pions' and used to determine the invariant mass of the pair and the decay vertex.

---

[1] Such a two-stage magnetic analysis might also be suited for measurement of inclusively produced charged hadrons or dilepton pairs.

5. APPARATUS AND EXPERIMENTAL RESOLUTION

The experimental set-up is shown in Fig.3. The polarized beam comes from the left and is defined in direction and impact point at the target by the fine-grained hodoscopes HB1, HB2 (with 1.5 or 1.0 mm wide, 5. mm thick scintillator elements).

For measurements of A_N and D we plan to use a liquid hydrogen target or a nuclear target. Also double- and triple-spin measurements with polarized targets might be performed, particularly if improvements in new polarizable materials (13) would turn out to be practical.

At short distance after the target is placed a multiplicity-sensitive detector (MSD) made of a high-resolution checkboard-shaped solid-state device [2] giving simultaneously the number of hit elements and the pulse amplitude from coincident particles on a single element.

The Λ^0 decay path (≈ 4. m) is defined between MSD and a proportional chamber module PC1 made of one vertical and two inclined (at 30° and -30°) sense wire planes. This geometry allows a simple determination of the space location of hits and their multiplicity. Two drift chamber modules (DC1,DC2) immediately behind PC1, measure the Λ^0 decay products' trajectories with high spatial resolution before entering the first magnet M1. A SCM105 magnet is suited for preliminarly resolving the p,π^- pair (according to charge) and for analyzing the pion momentum by measuring the outgoing direction by chambers DC3 and DC4.

The multicell Cerenkov counter C1 is used to tag the decay pions. The proportional chamber module PC2 defines a correlation between the allowed regions for the pions and the protons from Λ^0 decay.

---

[2] The possibility of making such detectors in the form of microstrip arrays has been demonstrated (14) and has important advantages, for precise position determination (< 1. mm), high rate capability (> 10^7 m.i. particles sec^{-1} cm^{-2}) and energy resolution (40 Kev FWHM for m.i.particles).

The second magnet M2 (BM109 type) further analyzes the momentum of the forward-going energetic protons which are then measured in a relatively small-aperture high-resolution proportional wire chamber telescope (PC3,PC4).

The Cerenkov counter C2 (7 m long) is used to tag the forward proton and the scintillation counter hodoscope H4 determines the track multiplicity and position in the second spectrometer at the end of the apparatus .

The effective mass and the momentum of the Λ^0 particles are reconstructed from the measured momenta and directions of the decay products. In the high-energy approximation :

$$M_\Lambda^2 \simeq m_p^2 + p_p p_\pi \theta_{p\pi}^2$$

$$p_\Lambda^2 \simeq (p_p + p_\pi)^2 - p_p p_\pi \theta^2$$

The Λ^0 direction is obtained with respect to the proton trajectory :

$$\theta_{\Lambda p} \simeq \theta_{p\pi} [p_\pi / (p_p + p_\pi)]$$

The experimental errors for the described set-up are :

$\Delta\theta_{p\pi} \simeq 0.2$ mrad for the decay opening angle measured before M1,

$\Delta p_\pi / p_\pi \simeq 6.2 \cdot 10^{-4}\, p_\pi$ for the π^- analyzed by M1 only,

$\Delta p_p / p_p \simeq 1.3 \cdot 10^{-4}\, p_p$ for the proton measured by both M1 and M2 .

In these experimental conditions, at a beam momentum $p_0 = 200$ Gev/c the precision in effective mass is $\Delta M_\Lambda \lesssim 70$ Mev FWHM at $x \simeq 0.8$ (30 Mev at $x \simeq 0.6$). The Λ^0 direction and momentum are measured with precisions :

$$\Delta\theta_\Lambda / \theta_\Lambda < 10\ \% \quad ; \quad \Delta p_\Lambda / p_\Lambda < 4\ \%$$

The kinematical variables $p_t \approx p_\Lambda \theta_\Lambda$ and $x \approx p_\Lambda / p_0$ for the process $pp \to \Lambda^0 X$ are therefore determined with precisions :

$$\Delta p_t / p_t \lesssim 10\ \% \qquad ; \qquad \Delta x / x \lesssim 6\ \%$$

6. TRIGGER CRITERIA AND ON-LINE SELECTION

The trigger is organized in two levels :

1. counter trigger using fast hardwired electronics ,
2. on-line event selection, using microprogrammable processors.

The counter trigger requires the following conditions :

- a beam particle signal, defined by the hodoscopes HB1, HB2 ;
- a preliminary 'neutral particle decay' tag in the region between hodoscopes H1, H2 obtained by comparing their multiplicities ;
- a correlation in space and time between decay protons and pions in hodoscopes H3 (allowing a multiplicity ≥ 2) and H4 ;
- a veto from counters A1, A2, A3 to suppress non-interacting beam particles ;
- a signature on the particle masses after the magnets M1 and M2 from multicell Cerenkov counters C1 and C2 .

The proposed settings of the Cerenkov counters are listed in Table I; for example at 200 Gev/c one expects C1 to accept both p and π^- from Λ^0's with $0.2 \lesssim x \lesssim 0.4$ and to ignore protons with momentum less than 32 Gev/c. C2 will refine this condition for events at large x . Therefore one expects to ignore a fraction larger than 50 % of the relatively low energy protons produced in multi-body reactions not involving neutral strange particles .

The counter trigger strobes the proportional and drift chambers and the MSD into the read-out system.

Fast microprogrammable processors (15) are then foreseen to refine the on-line selection using the MSD and proportional chamber information:

- the multiplicity N2 of points reconstructed on PC1 is compared to the multiplicity N1 measured in the MSD to check for the condition $N2 - N1 = 2$;
- further more complex correlations between hits in chambers PC1-PC3 according from the expected patterns of the decay pion and protons tracks can be imposed for the surviving events.

7. ACCEPTANCE EVALUATION AND BACKGROUND ESTIMATES

A Monte-Carlo program (16) is employed to determine the geometrical acceptance of the apparatus. Inclusive Λ^0 is generated with uniform distribution in phase-space with $0 \leq x \leq 1$ and $0. \leq p_t^2 \leq 6.$ $(Gev/c)^2$ at 200 and 400 Gev/c incident momentum.

The main factors influencing the acceptance are :

a) the available decay path for Λ^0 particles,

b) the vertical gap width of the magnet M1,

c) the solid angle for protons covered by M2.

These features of the set-up are in part subject to contradictory requirements as improving point a) would imply increasing the distance between the target and M1, while b) and c) are better matched by keeping the magnets close to the target.

To compromise between the three points the distances D1 and D2 have been adjusted to optimize the overall amount of accepted events, such that:

i) both proton and pion passed through the first magnet apertures,

ii) the forward proton reached the end of the apparatus.

The acceptance as a function of x and p_t^2 is given in Table II .

With the specified apertures for M1 and M2 the azimuthal acceptance for Λ^0 particles is larger than $\pm 50^0$ around the symmetric values $\phi = 0$ and $\phi = \pi$.

The Monte-Carlo program has also been employed to study the process $pp \to K^0(\to \pi^+\pi^-)X$ which is competing with Λ^0 production and leads in some cases to ambiguous definitions of the invariant mass.

The distinctive features of the K^0 decay are the relative distributions of momenta in the $\pi^+\pi^-$ pair which would allow to discriminate between Λ^0 and K^0 . Also the information of the Cerenkov counters together with momentum measurements would lead to separation of the two reactions.

It has been estimated that about 10 % of the events would give ambiguous results in the invariant mass evaluation.

The K^0 events should not be considered just as a background and there is the possibility of accepting a relevant fraction of them during data taking to measure their production asymmetry.

Background effects due to multi-body reactions can be appreciated by considering processes of multipion production with the average charged multiplicity $\langle n \rangle$ typical of the energy being considered and with uniform distribution in phase-space.

For example around 200 Gev/c $\langle n \rangle \simeq 8$ with a topological cross-section of 5 to 6 mbarn (17) and taking a representative reaction of the type $pp \to pp(N\pi^+)(N\pi^-)(M\pi^0)$ the overall acceptance of the set-up of Fig. 3 is about 3 %. The momenta spectra for protons and π^- are distinctly different from those of the Λ^0 decay.

The invariant mass distribution of all $p\,\pi^-$ pairs in the accepted events contributes about 1.4 % in the Λ^0 mass region. This gives an indication that events containing genuine vee-topologies can be sorted from a combinatorial background.

For what concerns the complication of such events, where an average number of 8 charged particles is associated to a Λ^0 or to a K^0 (18), we expect that the criteria of selection described at the end of chapter 4 and in the trigger section would appreciably speed up the pattern recognition procedure.

8. ESTIMATES OF RATES AND ASYMMETRY PRECISION

Using an experimental parametrization (19) of the differential cross-section for the reaction $pp \to \Lambda^0 X$, the number of events produced in each (x, p_t^2) bin is estimated for a beam of 10^7 polarized protons in a 20 second spill with 60 second repetition period, impinging on a 50 cm long liquid hydrogen target.

For one month running time (720 hours) the statistical accuracy ΔA_N achieved in the asymmetry measurement is shown in Fig. 4 as a function of x and p_t^2, assuming a 45 % beam polarization and a 1:2 background-to-signal ratio. Typical values for ΔA_N and ΔD_{NN} at $.25 \leq x \leq .75$ are :

p_t^2 =		.3 ± .06	2.2 ± .44	5. ± 1.	$(Gev/c)^2$
ΔA_N (%)	Λ^0	≈0.1	0.5	3.7	
	K^0	0.3	2.5	29.	
ΔD_{NN}(%)	Λ^0	0.2	1.0	8.	

A complete list of these accuracies is given in Table II as a function of x and p_t^2.

Systematic errors which might produce spurious asymmetries are suppressed by frequent flipping of the beam polarization and by changing the polarity of the spectrometer magnets and measuring the left-right asymmetries.

9. PLAN OF THE EXPERIMENT

We intend to start with the measurement of Λ^0 production with polarized proton beam and hydrogen target. We request 1600 hours of run time for:

a) System check and calibration	160 hours
b) A_N and D_{NN} measurements	720 hours
c) D_{LL} measurement	720 hours

The production rates and the detector acceptance allow some flexibility both in beam energy (between 200 and 400 Gev/c) and intensity.

Also data on K^0 production would be obtained during the same run periods; some information might be obtained on Σ^0 and Ξ^0 production using the photon detector proposed for the measurement of π^0 production with the polarized beam.

As a second stage measurement with the polarized antiproton beam could be performed around 200 Gev/c, where the spectrum of polarized $\bar{p}$ has a maximum ($3 \cdot 10^6$ per spill). To directly compare the results with incident protons and antiprotons it would be preferable to run also the first stage at 200 Gev/c.

We expect that polarized targets with optimized materials (having larger hydrogen content) would be available in the near future; in this

case also spin-spin correlations in the initial states and triple-spin parameters could be measured with the same apparatus in a third stage of the experiment.

It seems premature to establish a specific request for stages two and three now, but we can anticipate that periods comparable to stage one would be satisfactory.

It is likely that part of the setting-up (and hopefully part of the data taking) of this experiment could be performed simultaneously with other experiments proposed for the polarized beam.

REFERENCES

1. G.Bunce et al., Phys.Rev.Lett. 36 (1976) 1113.

   K.Heller et al.,Phys.Rev.Lett. 41 (1978) 607.

2. K.Heller et al.,Phys.Lett. 68B (1977) 480

   S.Erhan et al., Phys.Lett. 82B (1979) 301

   F.Lomanno et al., Phys.Rev.Lett. 43 (1979) 1905

   K.Raychaudhuri et al., Phys.Lett. 90B (1980) 319

3. I.P.Auer et al., Fermilab Proposal P581 (1978)

4. G.L.Kane,J.Pumplin and W.Repko, Phys.Rev.Lett. 41 (1978) 1689

5. D.Sivers,AIP Conference Proc. No.51, G.H.Thomas ed., Argonne 1978, p.505 .

6. A.Krzywicki,J.Engels,B.Petersson and U.Sukhatme, Phys. Lett. 85B (1979) 407.

7. F.E.Close and D.Sivers, Phys.Rev.Lett. 39 (1977) 1116.

   R.P.Bajpai and R.Ramachandran, Indian Institute of Technology Report, Kanpur (1980), submitted to Phys.Rev.Lett.

   K.Heller, University of Michigan Report UMHE 77-38 (1977)

   G.L.Kane and Y.P.Yao, Nucl.Phys. B137 (1978) 313

   A.C.Davis and R.J.A.Lambourne, Imperial College Report ICTP/78-79/4.

8. N.S.Craigie,F.Baldracchini,V.Roberto and M.Socolovsky, Trieste Int.Center for Theor.Physics Reports IC/80/96 (1980) and IC/80/148 (1980).

9. B.Andersson,G.Gustafson and G.Ingelman, Phys.Lett. 85B (1979) 417

   G.Gustafson, Talk presented at the 1980 Int.Symposium on H.E. Physics with Polarized Beams and Targets, Lausanne, LUTP 80-11 (1980).

10. T.A.DeGrand and H.I.Miettinen, University of Helsinki Report HU-TFT-80-47 (1980).

    H.I.Miettinen, Plenary Report at the Madison Conference (1980).

11. A.Lesnik et al., Phys.Rev.Lett. 35 (1975) 770

    R.Eisner et al., AIP Conf. Proc., M.Marshak ed., No.35 (1976) 210

12. J.F.Owens et al., Nucl.Phys. B112 (1976) 514

    J.F.Owens et al., Phys.Lett. 63B (1976) 341

13. T.O.Niinikoski, CERN-EP/80-227 (1980), talk presented at the 1980 Int. Symposium on H.E. Physics with Polarized Beams and Targets, Lausanne 1980.

    A.Abragam,V.Bouffard,Y.Roinel,P.Roubeau, DPh-G/SRM/80/1755 (1980), submitted to J.Phys.

14. E.H.M.Hejne et al., CERN Report CERN/EP/BEAM/80-6 (1980)

R.S.Amendolia et al., Pisa University and INFN report, Pisa 80-2 (1980).

G.P.Rancoita, private communication .

15. D.A.Jacobs, ESOP,a fast microprogrammable processor, Talk presented at the Europhysics Conf. on Computing in H.E. and nuclear Physics, Bologna (1980) and CERN/DD/80/22 (1980) .

16. based on the utility program GEANT, R.Brun et al., CERN/DD/78/2 .

17. S.Barish et al., Phys.Rev. D9 (1974) 2689

C.Bromberg et al., Phys.Rev.Lett. 31 (1973) 1563

A.Firestone et al., Phys.Rev. D10 (1974) 2080

18. K.Jaeger et al., Phys.Rev. D11 (1975) 2405

19. P.Skubic et al., Phys.Rev. D18 (1978) 3115 .

FIGURE CAPTIONS

Fig. 1 - Initial-final spin correlation for $\bar{p}p \to \Lambda^0 X$.

Fig. 2 - Distributions of kinematical quantities in the laboratory system for pions and protons from Λ^0 decay in $pp \to \Lambda^0 X$ at 200 Gev/c, versus Λ^0 momentum :

a) proton momentum

b) π^- momentum

c) opening angle.

Fig. 3 - Set-up for $pp \to \Lambda^0 X$:

HB1,2 beam hodoscopes, H1,2,3,4 trigger hodoscopes,

MSD multiplicity sensing detector

PC1,2,3,4 proportional chamber modules,

DC1,2,3,4 drift chamber modules

C1,C2 Cerenkov counters,

M1,M2 spectrometer magnets.

Fig. 4 - Equal-accuracy lines in phase-space (x, p_t^z) for $pp \to \Lambda^0 X$ at 200 Gev/c.

TABLES

TABLE I

Energy (Gev/c)	Counter	Gas	$(n-1)\cdot 10^6$	L(m)	E (Gev)	E (Gev)
200.	C1	CO_2	410.	3.5	4.5	32.
	C2	Air	290.	7.0	5.6	38.7
400.	C1	Ne	67.	3.5	15.	85.
	C2	He-Ne	54.	7.0	17.	105.

INCLUSIVE LAMBDA 0 AT 200. GEV/C BEAM 1.00E+07 P/SEC TARGET 50. CM

ACCEPTANCE (PER CENT)

XL \ PT2	0.	.12	.24	.36	.52	.80	1.18	1.78	2.66	4.00	6.00
.75	43.1	45.3	40.5	37.6	38.6	36.2	40.2	35.7	37.3	36.0	
.50	51.2	40.9	44.2	48.7	49.4	49.5	48.1	48.4	44.3	33.8	
.25	63.6	55.7	51.0	59.5	59.6	51.7	48.9	38.8	21.1	9.1	
0.00	57.3	54.4	39.2	33.3	22.8	12.2	4.8	2.6	.1	0.0	

ASYMMETRY ACCURACY

XL \ PT2	0.	.12	.24	.36	.52	.80	1.18	1.78	2.66	4.00	6.00
.75	2.29E-03	3.00E-03	4.09E-03	4.81E-03	5.27E-03	7.98E-03	1.22E-02	2.78E-02	8.06E-02	4.87E-01	
.50	1.16E-03	1.65E-03	1.95E-03	2.01E-03	2.08E-03	2.78E-03	4.02E-03	7.27E-03	1.80E-02	9.16E-02	
.25	7.56E-04	9.84E-04	1.23E-03	1.19E-03	1.18E-03	1.60E-03	2.16E-03	3.94E-03	1.09E-02	6.12E-02	
0.00	5.99E-04	7.27E-04	1.00E-03	1.12E-03	1.32E-03	2.18E-03	4.37E-03	9.04E-03	9.12E-02	0.	

INCLUSIVE LAMBDA 0 AT 400. GEV/C BEAM 1.00E+07 P/SEC TARGET 50. CM

ACCEPTANCE (PER CENT)

XL \ PT2	0.	.12	.24	.36	.52	.80	1.18	1.78	2.66	4.00	6.00
.75	25.7	17.2	27.6	28.6	22.8	22.0	21.0	24.4	22.4	22.3	
.50	29.9	28.8	25.3	38.8	27.1	32.7	30.3	31.1	30.5	30.1	
.25	44.6	49.5	38.3	58.2	42.4	41.5	42.3	43.1	38.5	38.0	
0.00	63.4	59.6	59.1	44.4	44.9	40.7	27.8	19.0	12.9	6.8	

ASYMMETRY ACCURACY

XL \ PT2	0.	.12	.24	.36	.52	.80	1.18	1.78	2.66	4.00	6.00
.75	2.96E-03	4.86E-03	4.94E-03	5.50E-03	6.83E-03	1.02E-02	1.68E-02	3.34E-02	1.03E-01	6.13E-01	
.50	1.51E-03	1.95E-03	2.56E-03	2.24E-03	2.79E-03	3.39E-03	5.01E-03	8.95E-03	2.14E-02	9.50E-02	
.25	8.91E-04	1.03E-03	1.39E-03	1.18E-03	1.38E-03	1.75E-03	2.26E-03	3.62E-03	7.78E-03	2.85E-02	
0.00	5.19E-04	6.31E-04	7.40E-04	8.77E-04	8.43E-04	1.07E-03	1.62E-03	2.96E-03	6.69E-03	2.96E-02	

Table II

INCLUSIVE K 0 AT 200. GEV/C BEAM 1.00E+07 P/SEC TARGET 50. CM

ACCEPTANCE (PER CENT)

XL \ PT2	0.	.12	.24	.36	.52	.80	1.18	1.78	2.66	4.00	6.00
.75	50.0	52.5	48.0	47.5	39.8	43.9	45.9	45.9	47.2	44.6	
.50	58.8	52.2	61.2	49.6	52.7	51.5	52.3	55.3	48.5	38.3	
.25	60.9	62.1	58.2	61.3	58.1	54.7	49.0	36.7	21.5	12.1	
0.00	29.1	27.4	15.0	23.0	11.5	7.5	7.1	4.2	1.2	.7	

ASYMMETRY ACCURACY

XL \ PT2	0.	.12	.24	.36	.52	.80	1.18	1.78	2.66	4.00	6.00
.75	1.85E-02	2.48E-02	3.34E-02	3.77E-02	4.51E-02	6.22E-02	9.88E-02	2.25E-01	7.35E-01	4.55E+00	
.50	4.20E-03	5.80E-03	6.65E-03	8.04E-03	8.22E-03	1.15E-02	1.75E-02	3.61E-02	1.18E-01	7.25E-01	
.25	1.24E-03	1.52E-03	1.88E-03	1.94E-03	2.02E-03	2.75E-03	4.24E-03	9.80E-03	3.65E-02	2.44E-01	
0.00	5.25E-04	6.57E-04	1.06E-03	9.06E-04	1.30E-03	2.11E-03	3.12E-03	7.92E-03	4.09E-02	2.51E-01	

INCLUSIVE K 0 AT 400. GEV/C BEAM 1.00E+07 P/SEC TARGET 50. CM

ACCEPTANCE (PER CENT)

XL \ PT2	0.	.12	.24	.36	.52	.80	1.18	1.78	2.66	4.00	6.00
.75	31.0	30.8	23.0	25.7	28.2	28.1	28.5	27.3	26.1	28.3	
.50	32.8	32.0	28.2	37.2	33.1	36.8	35.7	36.6	36.7	38.0	
.25	52.3	36.2	47.9	54.6	53.1	53.4	51.6	52.0	48.3	41.0	
0.00	56.9	45.9	43.4	39.9	39.7	36.1	29.3	21.3	14.0	8.0	

ASYMMETRY ACCURACY

XL \ PT2	0.	.12	.24	.36	.52	.80	1.18	1.78	2.66	4.00	6.00
.75	2.35E-02	3.24E-02	4.82E-02	5.12E-02	5.35E-02	7.76E-02	1.25E-01	2.90E-01	9.81E-01	5.65E+00	
.50	5.61E-03	7.40E-03	9.77E-03	9.26E-03	1.03E-02	1.35E-02	2.10E-02	4.39E-02	1.34E-01	7.15E-01	
.25	1.33E-03	1.98E-03	2.06E-03	2.04E-03	2.09E-03	2.74E-03	4.05E-03	8.00E-03	2.34E-02	1.26E-01	
0.00	3.45E-04	4.63E-04	5.66E-04	6.20E-04	6.26E-04	8.55E-04	1.36E-03	3.09E-03	1.04E-02	6.52E-02	

Table I I. A

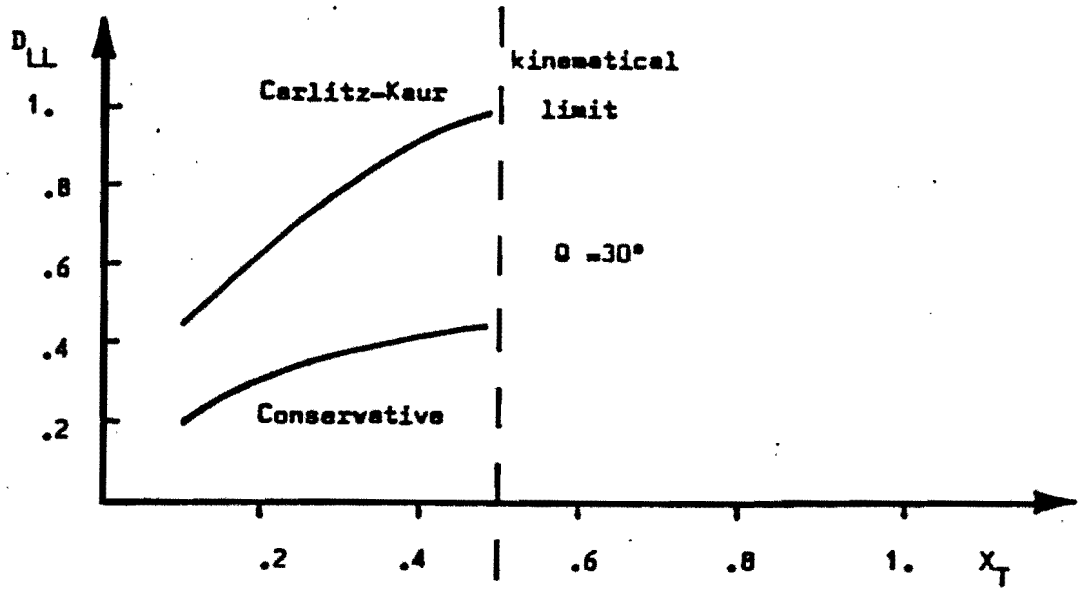

Predictions for $\bar{P}\,P \longrightarrow \Lambda^0 X$ (Ref.8)

$S = 1000\ GeV^2$

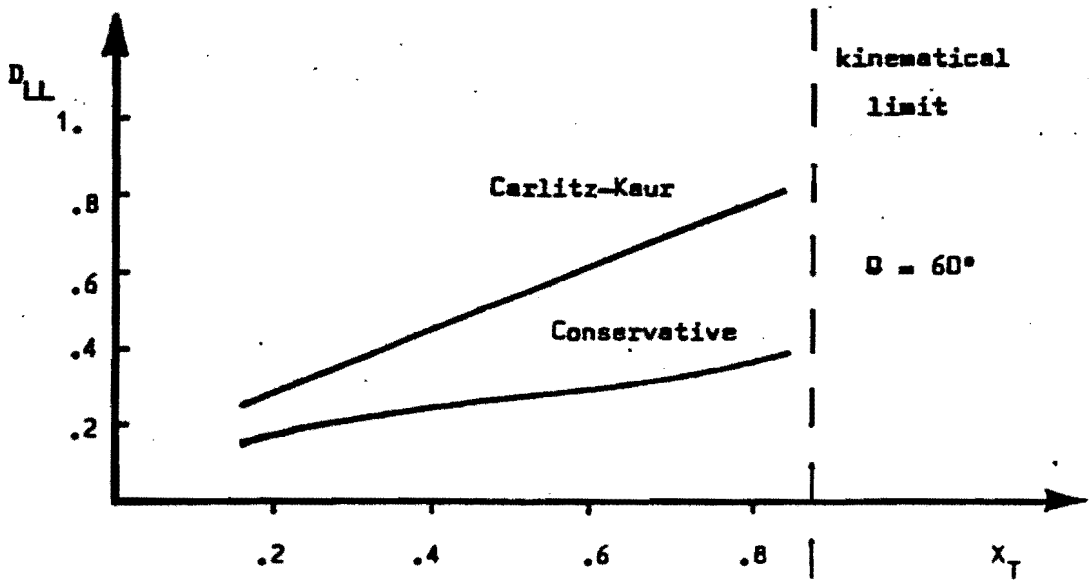

Fig.1

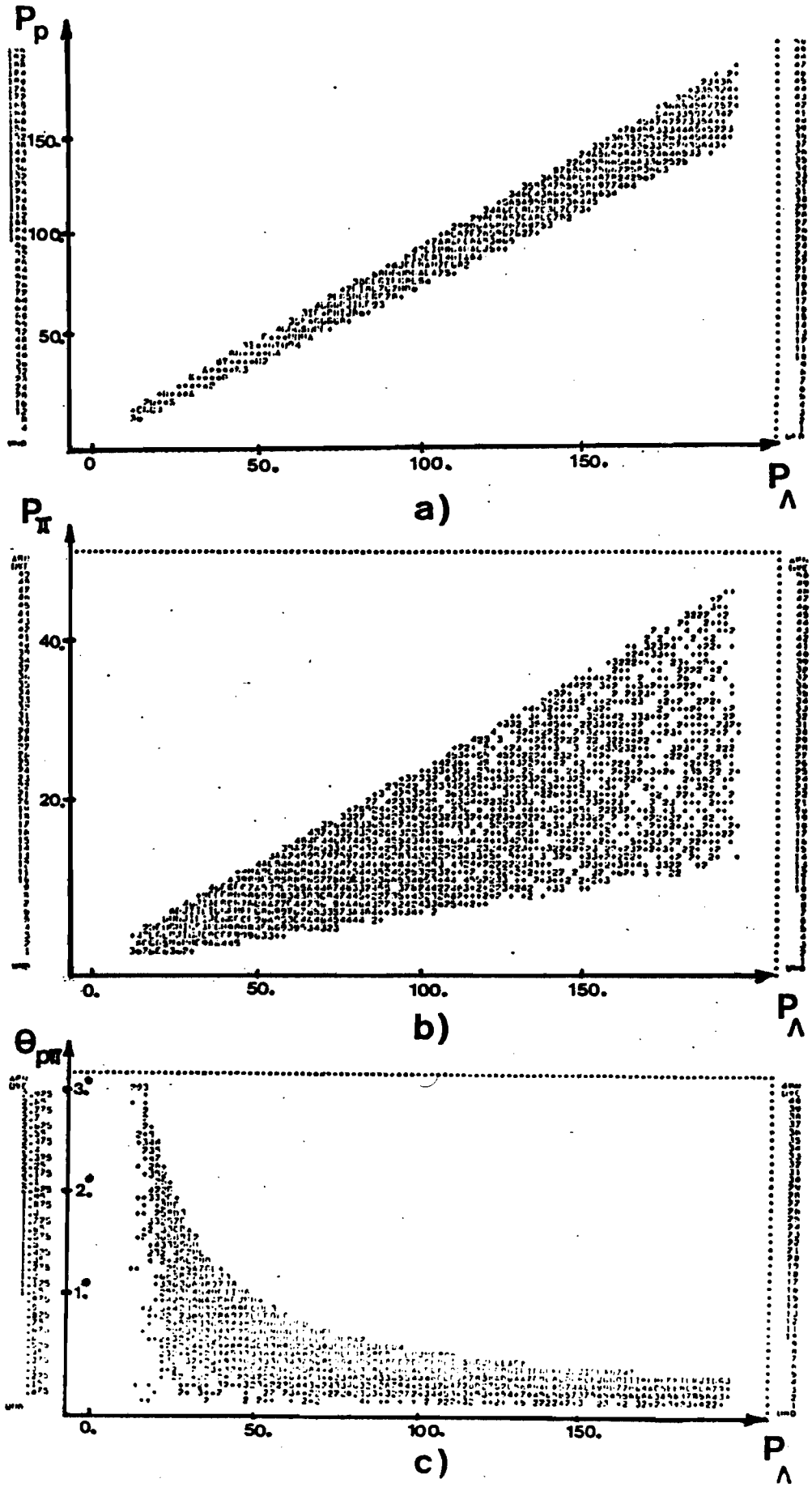
P_p
150.
100.
50.
0
50.
100.
150.
P_Λ
a)
P_π
40.
20.
0.
50.
100.
150.
P_Λ
b)
$\theta_{p\pi}$
3°
2°
1°
0.
50.
100.
150.
P_Λ
c)

Fig. 2

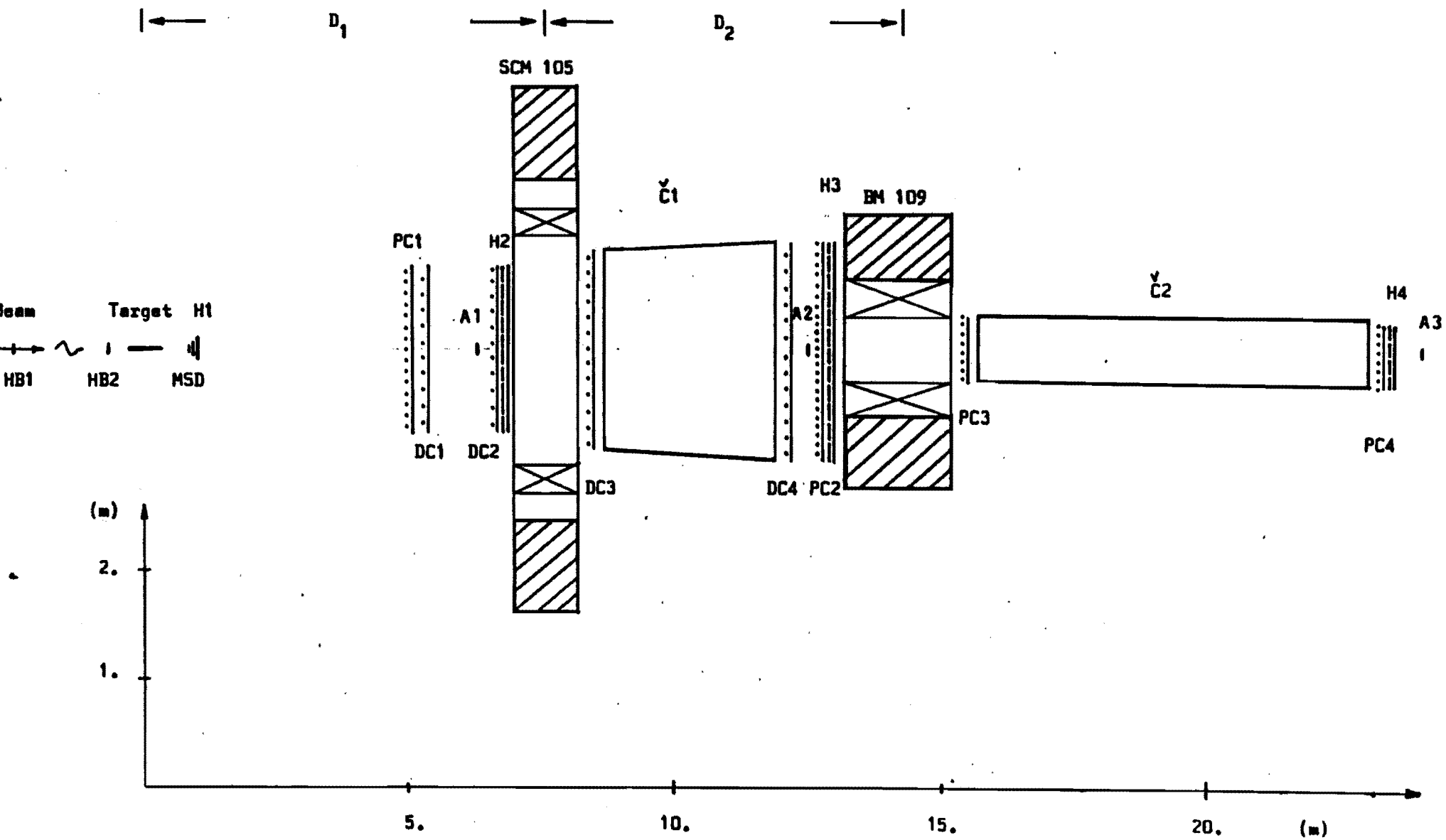
D1
D2
SCM 105
Čl
H3
BM 109
PC1
H2
A1
Beam
Target
H1
HB1
HB2
MSD
DC1
DC2
DC3
DC4
PC2
A2
PC3
Č2
H4
A3
PC4
(m)
2.
1.
5.
10.
15.
20.
(m)

Fig.3.

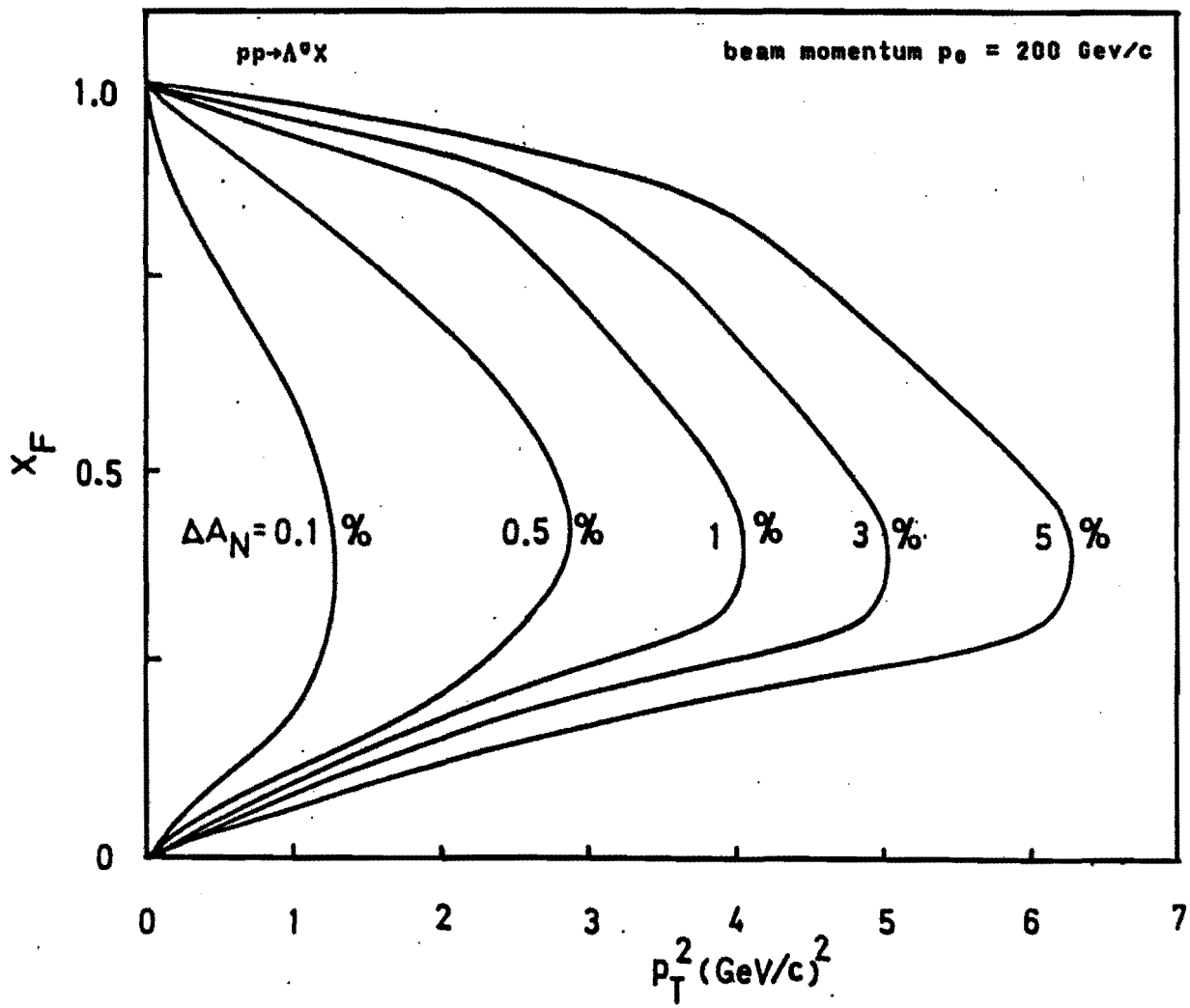
pp→Λ°X
beam momentum p₀ = 200 Gev/c
1.0
0.5
0
x_F
ΔA_N= 0.1 %
0.5 %
1 %
3 %
5 %
0
1
2
3
4
5
6
7
p_T^2 (GeV/c)^2

Fig. 4